MICROSTRUCTURE AND MECHANICAL PROPERTIES OF ALUMINUM AND A356 ALLOY FOAMS CRYSTALLIZED IN A THIN-WALLED WATER-COOLED MOLD

Rositza Dimitrova[1], Tatiana Simeonova[1,2],
Boyko Krastev[1], Angel Velikov[1], Valentin Manolov[1]

[1]*Bulgarian Academy of Sciences*
Institute of Metal Science, Equipment and Technologies
with Hydro- and Aerodynamics Centre "Acad. A. Balevski",
67 Shipchenski Prohod Blvd., Sofia 1574, Bulgaria
[2]*Bulgarian Academy of Sciences, Institute of Mechanics,*
Acad. Georgi Bonchev St., Bl. 4, Sofia 1113, Bulgaria
E-mail: rossy@ims.bas.bg

Received: 25 January 2024
Accepted: 06 March 2024
DOI: 10.59957/jctm.v59.i3.2024.23

ABSTRACT

Cylindrical foam castings of Al and A356 alloy were produced using a melt foaming method with the introduction of Ca and TiH_2. Foam crystallization takes place in a cooled thin-walled metal mold. Samples cut off from the foam castings are investigated by X-ray tomography, quantitative data for porosity, average pores diameter and average cells wall thickness are obtained. It is found that the porosity is mainly open. Same samples are tested in quasi-static mode and the compressive strength is determined. The influence of porosity on compressive strength is analyzed.

Keywords: metal foams, Al and Al alloy foam castings, computed tomography (CT) analysis, compressive strength.

INTRODUCTION

Solid metal foams are new functional materials, which are of big interest in the past years due to their unique combination of physical and mechanical properties, such as high stiffness with very low specific weight and high gas permeability and conductivity. Because of their properties they are used in many industrial sectors (automotive, railway, building and aerospace industry, ship building, biomedical industry etc.) [1]. Production, determination of characteristics and application of metal foams with open or closed porosity is presented comprehensively in [1 - 3]. One of the main methods for obtaining metal foams is by introducing a foaming agent into the melt of pure metal /metal alloy, applied in the current study as well [7, 8]. Among the non-destructive methods for characterizing cellular materials is X-ray computed tomography (CT) method [1], which is used in many investigations [4 - 6, 9 - 11]. X-raying the samples and post-processing the projection images allows to calculate the open, closed and total porosity, as well as to determine the pores diameter and their percent volume in range, and the wall thickness. Another important characteristic, the compressive strength, is the subject of extensive research [12, 13]. It is shown that there is a dependence of the compressive strength on the relative density. This allows this mechanical property to be predicted if the relative density is known. Recently, aluminum alloy foams and in particular A356 alloy are investigated. This alloy has good casting properties, resistance to corrosion and weldability, and is used for production of structural elements. Movahedi et al. presented results on the influence of melt temperature on the mechanical properties of A356 alloy foam [14]. An important feature of the foam, thermal conductivity coefficient of A356 alloy foam is determined by mathematical modeling [15]. Usually, the published works are focused on the study of foams

of Al or Al alloys. In the present work using the same experimental apparatus foam castings of Al and A356 alloy are obtained. A comparison of their properties is done.

EXPERIMENTAL

Used materials and casting technology

Al and A356 alloy are manufactured by Stam Trading Ltd. Chemical composition of Al and A356, obtained through optical emission spectrometer Q4 Tasman Q101750 - C 130, Bruker is given in Table 1.

TiH_2 is manufactured by AG MATERIALS INC, Taiwan. Ca is manufactured and supplied by Alfa Aesar, Thermo Fisher (Kandel) GmbH Germany.

A statistical distribution of the particle dimensions of TiH_2 foaming agent, is obtained through Analysette22 NanoTec plus apparatus. Particle size distribution curves Q3(x) and their derivatives dQ3(x) as a function of particle size (x) are given in Fig. 1. The mean particle size is 28.9 μm.

Technology for obtaining foam castings includes the following stages:

- Melting of 2 kg Al or A356 alloy in a resistance furnace.
- Introduction of 2.5 wt.% Ca into the melt to increase its viscosity. For Al the temperature of introduction is 690ºC, and for A356 alloy - 650ºC.
- Intensive stirring for homogenization of Ca in the melt. The stirring speed is 600 rpm for 6 min for both Al and A356 alloy melts.
- Pouring the melt into a thin-walled metal form with inner diameter of 130 mm, located in a second resistance furnace heated to 655ºC.
- Introduction of 1.5 wt.% foaming agent - TiH_2 powder.
- Intensive stirring for TiH_2 homogenization in the melt with stirring speed of 850 rpm for 90 s for both Al and A356 alloy melts.
- Decomposition of TiH_2, followed by separation of H_2 and foaming, where the melt volume increases as a result of pores formation.
- Removing the metal form outside the furnace. Cooling of the outer wall by jets of water flowing from a ring located at the top of the metal form. The water temperature is 150ºC, cooling time - 6 min, water flow rate - 3.5 l/min.

Cylindrical foam castings with a diameter of

Table 1. Chemical composition of Al and A356, obtained through optical emission spectrometer Q4 Tasman Q101750-C 130, Bruker.

Material	Si, wt.%	Fe, wt.%	Cu, wt.%	Mg, wt.%
Al	0.075	0.103	≤ 0.002	0.012
A356	9.28	0.487	0.055	0.326

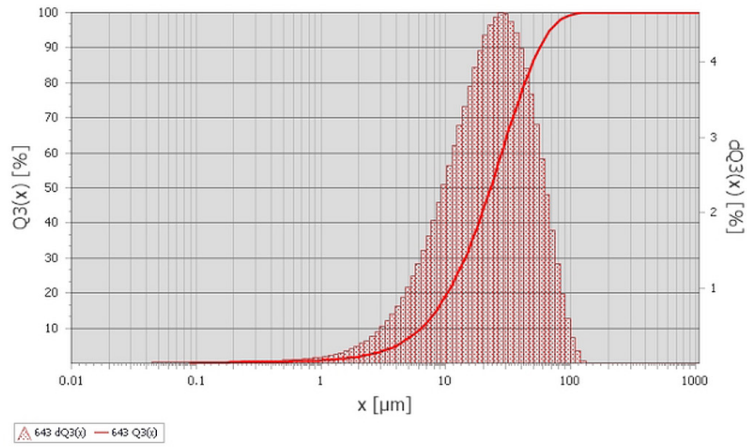

Fig. 1. TiH_2 particle size distribution curves Q3(x) and their derivatives dQ3(x) as a function of particle size (x).

130 mm and heights for aluminum - 212 mm and for alloy A356 - 247 mm, are obtained. Samples with dimensions of 18x18x18 mm are cut from the foam molds. 8 mm thick surface layer is not sampled due to the high crystallization rate and low porosity of the casting. The coordinates of the center of each sample R and Z are the radius and height measured from the vertical axis of symmetry and from the bottom of the casting, respectively. The coordinate values are listed in Table 2.

Measuring the density

Density of the obtained foam castings of Al and A356 alloy foams is determined by measuring their weight and the volume of water displaced by it, using the Archimedes' principle. To prevent the penetration of water into the pores, the castings surface is covered with a waterproof film during the measurements. The obtained data are compared to CT analysis data.

CT analysis

Samples of Al and A356 alloy foam castings are scanned by X-ray microtomograph SkyScan 1272, Bruker. The irradiation settings are: resolution 2452x1640 pxl, image pixel size: 10.885958 μm, rotation step: 0.200º, 360º rotation of sample, filter: Al 0.5 + Cu 0.038. X-ray projection images are processed and reconstructed with NRecon software. CTVox software is used to visualize the obtained model, and CTAn software - for receiving quantitative data, i.e. percentage of open, closed and total porosity, pores diameters and wall thickness.

Mechanical characterization

Samples from both materials are studied in order to obtain their mechanical properties under quasi-static compression. The experiments are conducted on servo-hydraulic testing machine ZwickRoell HA - 250 at a strain rate of 0.001 s^{-1}.

RESULTS AND DISCUSSION

Visualizations of foam casting samples in a selected section, top view, with CTVox software are given in Fig. 2 and Fig. 3. The scale bar is provided in the top left corner of the images.

According to the CT analysis data, given in Table 2, Al and A356 alloy foam samples have mainly open

Table 2. CTAn analysises quantitative data of samples, with indicated coordinates and local time of crystallization of the samples, calculated by CTAn software.

Sample	Position data	Local time of crystallization τ, s	Open porosity, %	Total porosity, %	Average diameter of pores, mm	Average thickness of walls, mm
Al-1	R = 47.5 mm Z = 120 mm	1.55	60.25	60.605	1.32 ± 0.58	0.893 ± 0.276
Al-2	R = 28.5 mm Z = 120 mm	3.84	74.4	74.703	2.39 ± 0.99	0.875 ± 0.199
Al-3	R = 9.5 mm Z = 120 mm	15.1	77.562	78.002	2.88 ± 1.48	0.994 ± 0.282
Al-4	R = -9.5 mm Z = 120 mm	15.1	84.92	84.936	1.79 ± 0.66	0.414 ± 0.113
A356-1	R = 47.5 mm Z = 120 mm	14.59	76.282	76.38	1.56 ± 0.68	0.631 ± 0.141
A356-2	R = 28.5 mm Z = 120 mm	28.07	77.665	77.867	1.57 ± 0.69	0.501 ± 0.131
A356-3	R = 9.5 mm Z = 120 mm	37.4	82.35552	82.578	2.38 ± 1.03	0.637 ± 0.134
A356-4	R = - 9.5 mm Z = 120 mm	37.4	83.03077	83.104	2.22 ± 0.92	0.529 ± 0.131

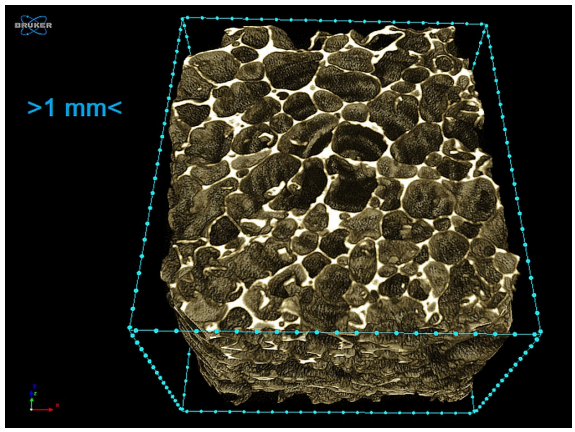

Fig. 2. CTVox visualization of Al foam sample.

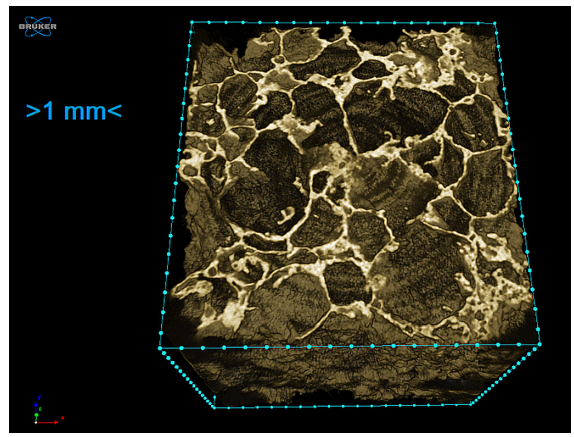

Fig. 3. CTVox visualization of A356 alloy foam sample.

porosity and a very low percentage of closed porosity. Al samples porosity is ranged from 60.6 % to 84.9 %. For A356 alloy samples, the porosity is ranged from 76.38 % to 83.1 %.

The densities of obtained foam castings of Al and A356 alloy foams, determined by Archimedes' principle, are $0.71.10^3$ kg m^{-3} and $0.61.10^3$ kg m^{-3}, respectively. As known, pure aluminum and aluminum-based alloys have a density of $2.7.10^3$ kg m^{-3}. Thus, as a result of foaming, the density is reduced from 3 to 4.4 times. According to these data the average porosity of Al and A356 alloy foams is 74 % and 77 %. The lower measured porosity values compared to those determined by CT analysis can be explained by the presence of a low porosity surface layer in the castings which was not sampled.

Considering the location of the Al samples (R in the second column in Table 2), it can be concluded that there is a tendency for porosity to increase from the periphery of the casting to the center. For A356 alloy samples, we have a less pronounced trend. Table 2 presents also the local crystallization times for the respective samples. They are calculated using a mathematical model of foam casting crystallization described in work [15]. There is an analogous trend with the increase of crystallization local time the porosity increases too. The average pore diameter for Al samples is in the range from (1.32 ± 0.58) mm to (2.88 ± 1.48) mm, and for A356 - from (1.56 ± 0.68) mm to (2.38 ± 1.03) mm, with "±" is given the standard deviation. In Fig. 4 and Fig. 5 pore size distribution and accumulation fraction dependence for one Al sample and one A356 alloy sample are shown.

As can be seen from the figures for Al sample the average pore size distribution changes from 0.25 mm to 5.75 mm, and for A356 alloy sample - from 0.25 mm to 3.75 mm. These results are obtained at the same Ca and TiH_2 concentrations, casting weight and mold geometry. This may be due to the presence of the alloying elements in the alloy and the lower crystallization temperature. From the function of the accumulative part, it can be concluded that the slope of the curves for Al sample is U = 18 % mm^{-1} and for A356 sample, respectively U = 35 % mm^{-1}. As it is known, this value determines the homogeneity of the foam. The larger it is, the more homogeneous is the foam. For comparison, Shi et al. described that this value for Al varies in the range from 13 to 55 for different types of samples obtained under different initial conditions [13].

The compressive strength of tested pure Al and A356 alloy samples is presented in Fig. 6 and Fig. 7, respectively. Additionally, compression properties corresponding to 20 % and 30 % deformation of both tested materials are shown in Table 3.

It is evident from the results that the increase of porosity (P) leads to decrease of the compressive strength (σ) of investigated materials. The dependences of the compressive strength as a function of materials porosity σ = f{P} for Al samples (curve 1) and A356 alloy samples (curve 2) are presented in Fig. 8.

As can be seen the strength of A356 alloy foam is about 15% higher than that of Al at a porosity of 75 %, and

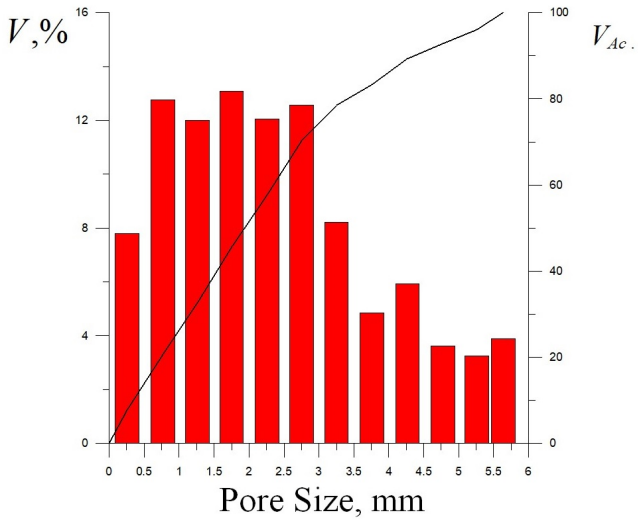

Fig. 4. Pore size distrbution and accumulative fraction, for sample Al-3.

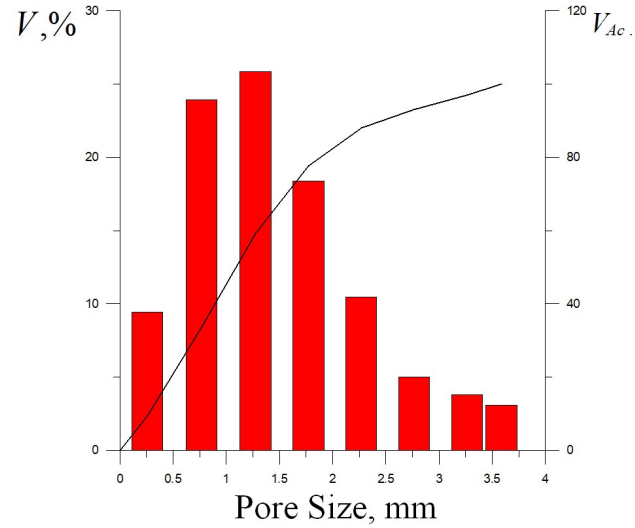

Fig. 5. Pore size distrbution and accumulative fraction, for sample A356-2.

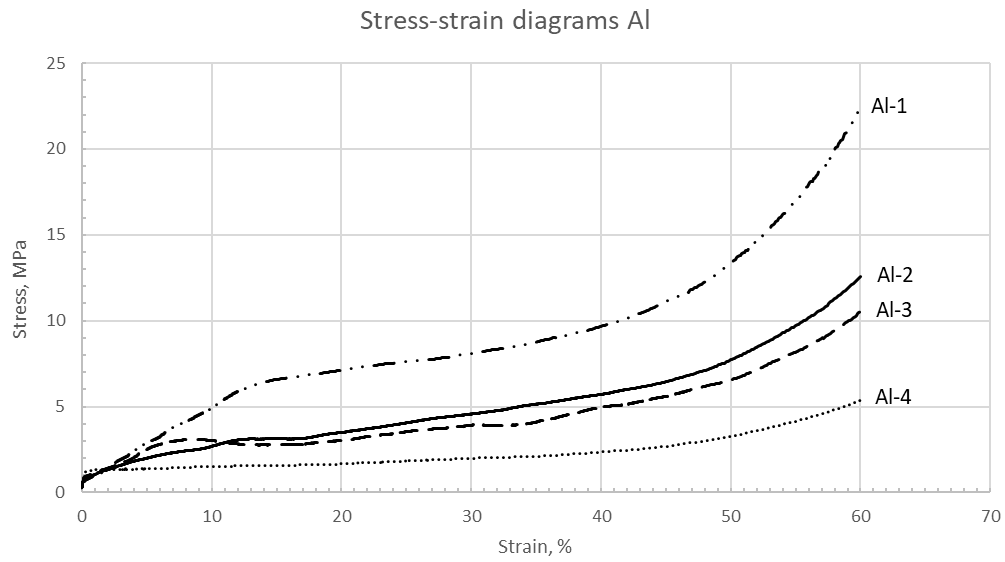

Fig. 6. Stress-strain diagram of Al foam samples Al-1, 2, 3, 4.

Table 3. Porosity and compressive stress data for Al and A356 alloy foam samples, calculated by CTAn software.

Sample	Porosity, %	σ (20 %), MPa	σ (30 %), MPa	Compressive strength, MPa
Al-1	60.605	7.11	8.11	22.4
Al-2	74.703	3.49	4.57	12.56
Al-3	78.002	3.01	3.91	10.54
Al-4	84.936	1.66	1.99	5.4
A356-1	76.38	4.18	4.76	17.8
A356-2	77.86	3.55	3.55	9.1
A356-3	82.578	2.73	3.34	5.4
A356-4	83.104	1.66	2.02	3.4

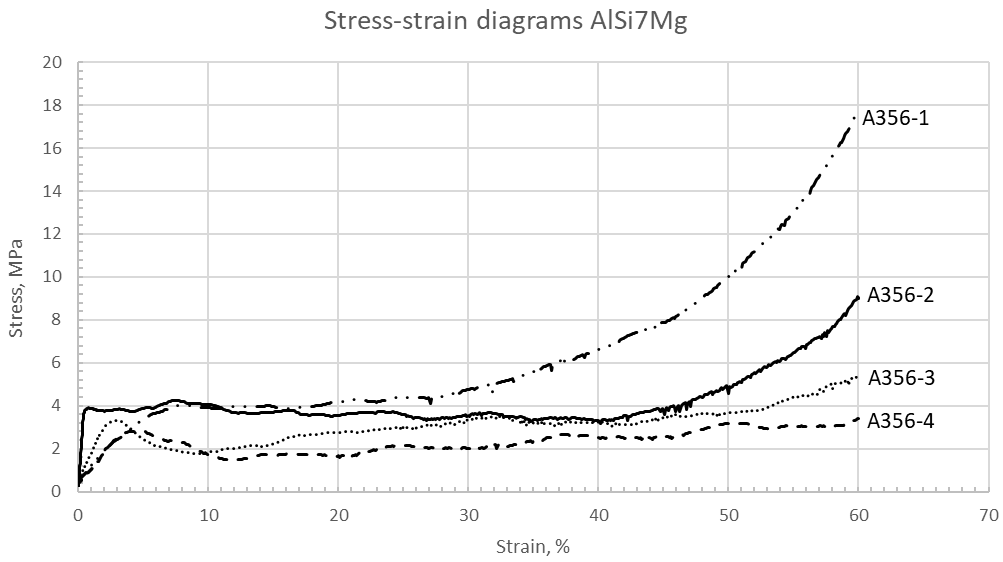

Fig. 7. Stress-strain diagram of A356 alloy foam samples A356-1, 2, 3, 4.

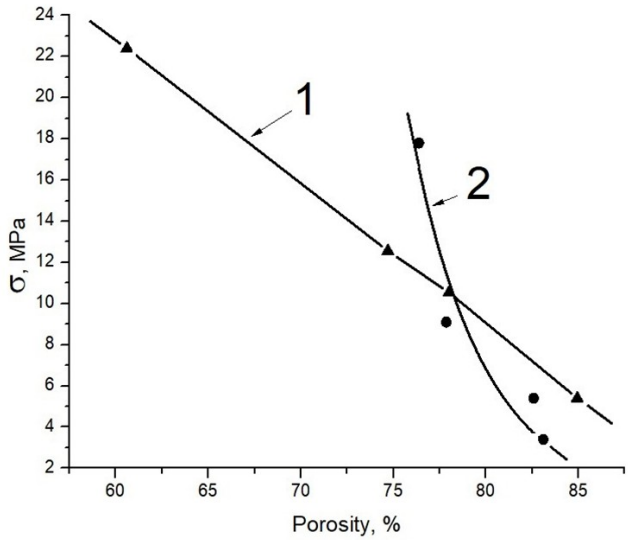

Fig. 8. Comparison of foam strength as a function of porosity σ= f{P} for Al samples (curve 1) and for A356 alloy samples (curve 2).

at a porosity above 80 % it is lower than the strength of Al foam. It means that at higher porosities higher strength values aren't obtained for alloy A356 compared to those of Al foam. According to the Gibson-Ashby models, the plateau stress depends on the foam relative density ρ_{rel}= (1-P)/100 and can be determined by the formulas for open pore (1) or for closed pore (2) materials [16, 17]:

a) for open pores $\sigma_{pl} = \sigma_{ys} C \rho_{rel}^{3/2}$ (1)

b) for closed pores $\sigma_{pl} = \sigma_{ys} C \rho_{rel}^{1.95}$ (2)

where σ_{pl} is the plateau stress, σ_{ys} is the yield strength, ρ_{rel} is the relative density, and the constant C is a shape factor that contains all the constants of proportionality, with value of 0.3 for open pore and 1.21 for closed pore materials.

Shi et al. reported that the yield strength of σ_{ys}= 100 MPa is obtained for Al modified with 2 % Ca, but the value is corrected and σ_{ys} = 127 MPa is

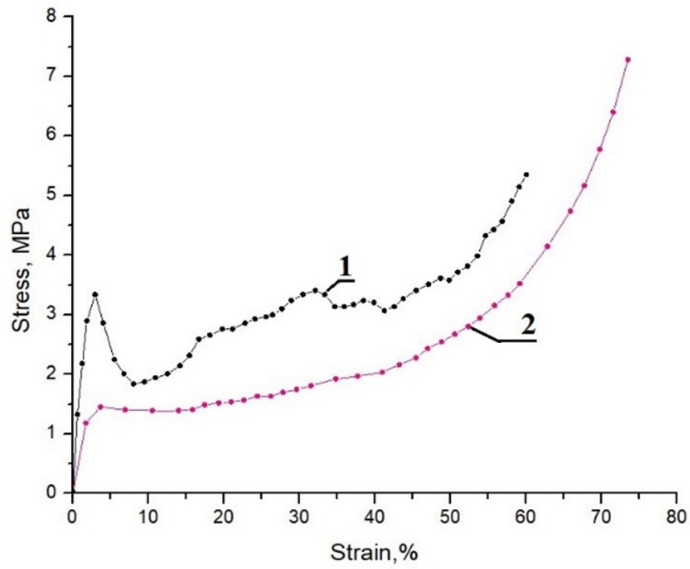

Fig. 9. Comparison of stress-strain diagrams of A356 alloy foams with a porosity of 82.5 % obtained in the present work (curve 1) and the results from [19] with a porosity of 80 % (curve 2).

Table 4. Comparison of experimentally measured and calculated by the Gibson–Ashby formula [16, 17] plateau stresses of Al foam samples.

Sample	Porosity, %	$\overline{\sigma_{pl}}$, MPa	σ_{pl}, MPa open	σ_{pl}, MPa closed
Al-1	60.605	7.61	7.58	18.4
Al-2	74.703	4.03	3.97	7.96
Al-3	78.002	3.46	3.0	5.74
Al-4	84.936	1.825	1.74	2.72

accepted [13]. According to received by us stress-strain diagram for Al modified with 2.5 % Ca, yield strength of σ_{ys} = 91 MPa is determined. The calculations made according to the above formulas for open and closed porematerials and the results from experimental measurements are presented in Table 4 for comparison.

The values $\overline{\sigma_{pl}}$ are determined by the stress-strain diagrams for Al samples in the interval σ_{20}- σ_{30} (averaging the stresses between 20 % and 30 % deformation) according to the standard [18]. Relatively good agreement between measured and calculated results for open porosity is obtained. As stated above (Table 2), CT analysis results showed that the investigated materials porosity is mainly open. A comparison of our results for open-porosity foam with the stress-strain curves of closed-porosity Al foam with a relative density of 0.105 obtained with described by Miyoshi et al. is also done [12]. The strength in the plateau region is about 2.5 MPa, while the measured strength of our Al foam sample with a relative density of 0.151 is 1.82 MPa. This is due to the different types of porosity. A comparison of the compressive strength of A356 alloy foam, obtained in this study and those reported by Zhang et al. at close values of porosity of samples - 82.578 % and 80 %, respectively, is presented in Fig. 9 [19].

As can be seen, the compressive strength data of our material exceed those obtained by Zhang et al., despite the closed porosity of the studied samples [19]. Likely, other factors except porosity affect this important property of foams.

CONCLUSIONS

- The porosity determined by CT analysis changes from the casting surface to the central axis of symmetry as follows: for Al casting foam samples from 60 % to 84.936 %, and for A356 alloy casting foam samples - from 76 % to 83.104 %. i.e. there is a tendency for porosity to vary depending on the location of the sample. The average pore diameter for Al foam casting foam samples varies between (1.32 ± 0.58) mm and (2.88 ± 1.48) mm and average cell wall thickness is in the range of (0.414 ± 0.113) mm to (0.994 ± 0.282) mm. For A356 alloy foam casting samples, the same parameters are respectively: from (1.56 ± 0.68) mm to (2.38 ± 1.03) mm and from (0.501 ± 0.131) mm to (0.637 ± 0.134) mm.
- The compressive strength of tested samples decreases with the increase of the porosity, as expected. Depending on the porosity, the compressive strength of Al casting foam samples varies from 5.4 MPa to 22.4 MPa, and for A356 alloy casting foam samples - from 3.4 MPa to 17.8 MPa. Results, which are shown in Table 3 and Fig. 8 lead to the conclusion that for lower porosities, the compressive strength of A356 alloy foams is higher compared to Al foams. At higher porosities, A356 alloy foam strength is lower or equal to the strength of Al foam.
- The measured plateau stresses of Al foam are compared with the Ashby model for open porosity materials. A satisfactory match was obtained (Table 4) with the dependence $\sigma_{pl} = \sigma_{ys} C \rho_{rel}^{3/2}$ (C = 0.3 and σ_{ys} = 91 MPa). The comparisons with other authors show that our results objectively represent the properties of the obtained foam materials.

Acknowledgements

This work is supported by a project under contract No КП-06-H47/12, funded by the Bulgarian Scientific Research Fund at Ministry of Education and Science, Bulgaria. Micro CT system SkyScan 1272, Bruker, Optical emission spectrometer Q4 Tasman Q101750-C 130, Bruker and servo-hydravlic testing machine Zwick Roell HA - 250 are purchased under Project BG05M2OP001-1.001-0008 "National Center for Mechatronics and Clean Technologies" funded by EU Operational Program "Science and Education for Smart Growth" 2014-2020.

REFERENCES

1. J. Banhart, Manufacture, characterisation and application of cellular metals and metal foams, Progress Mat. Sci., 46, 6, 2001, 559-632.
2. S. Kim, Chang-Woo, A review on manufacturing and application of open-cell metal foam, Proc. Mat. Sci., 4, 2014, 305-309. doi:10.1016/j.mspro.2014.07.562.
3. A. Kulshreshtha, S.K. Dhakad, Preparation of metal foam by different methods:A review, Mat.Today: Proceedings, 26, 2020, 1784-1790. https://doi.org/10.1016/j.matpr.2020.02.375
4. Fr.Garcı´a-Moreno, P.H. Kamm, T.R. Neu, J. Banharta, Time-resolved insitu tomography for the analysis of evolving metal-foam granulates, J. Syn. Rad., 25, 2018, 1505-1508. https://doi.org/10.1107/S1600577518008949
5. J. Bock, A.M. Jacobi, Geometric classification of open-cell metal foams using X-ray micro-computed tomography, Mat. Charact., 75, 2013, 35-43. http://dx.doi.org/10.1016/j.matchar.2012.10.0
6. D. Miedzinska, T. Niezgoda, R. Gieleta, Numerical and experimental aluminum foam microstructure testing with the use of computed tomography, Comp. Mat. Sci., 64, 2012, 90-95. doi:10.1016/j.commatsci.2012.02.021
7. S. Sowmiyaa, P. Nallanukalab, J. Anburaja, B. Simhachalamb, Development of Metallic Aluminium Foam Casting Using Calcium Carbonate Precursors for Side Impact Beam Application, Mat. Today: Proc., 5, 2018, 20362-20370. https://doi.org/10.1016/j.matpr.2018.06.411
8. D.P. Mondal, N. Jha, B. Gull, S. Das, A. Badkul, Microarchitecture and compressive deformation behavior of Al-alloy (LM13) - cenospherehybrid Al - foam prepared using $CaCO_3$ as foamingagent, Mat. Sci.&Eng. A, 560, 2013, 601-610. http://dx.doi.org/10.1016/j.msea.2012.10.003
9. E. Hamidi, P. Ganesan, S.V. Muniandy, M.H. Hassan, Lattice Boltzmann Method simulation of flow and forced convective heat transfer on 3D microX-ray tomography of metal foam heatsink,

Int. J. Th. Sci., 172, 107240, 2022, 1-21. https://doi.org/10.1016/j.ijthermalsci.2021.107240

10. Q. Fly, M. Meyer, F. Whiteley, T. Iacoviello, P.R. Neville, D.J.L. Shearing, C. Brett, R. Kim, Chen, X-ray tomography and modelling study on the mechanical behaviour and performance of metal foam flow-fields for polymerelectrolyte fuel cells, Int. J. Hyd. En., 44, 2019, 7583-7595. https://doi.org/10.1016/j.ijhydene.2019.01.206
11. Y. Wu, X. Lu, J.I.S. Cho, L. Rasha, M. Whiteley, T.P. Neville, R. Ziesche, N. Kardjilov, H. Markotter, I. Manke, X. Zhang, P.R. Shearing, D.J.L. Brett, Multi-length scale characterization of compression on metal foam flow-field based fuel cells using X-ray computed tomography and neutron radiography, En. Conv. Man., 230, 2021, 1-10. https://doi.org/10.1016/j.enconman.2020.113785
12. T. Miyoshi, M. Itoh, S. Akiyama, A. Kitahara, Aluminum Foam"ALPORAS": The Production Process, Propertiesand Applications, Mat. Res. Soc. Symp. Proc., 521, 1998.
13. T. Shi, X. Chen, Y. Cheng, Y. Liu, H. Zhang, Y. Li, Microstructure and Compressive Properties of Aluminum Foams Made by 6063 Aluminum Alloy and Pure Aluminum, Mat. Trans., 59, 4, 2018, 625-633. https://doi.org/10.2320/matertrans.M2017300
14. N. Movahedi, S.M.H. Mirbagheri, S.R. Hoseini, Effect of foaming temperature on the mechanical properties of produced closed-cell A356 Aluminum foams with melting method, Met. Mater. Int., 20, 4, 2014, 757-763. doi: 10.1007/s12540-014-4021-2
15. G. Georgiev, A. Velikov, B. Krastev, S. Popov, S. Stanev, R. Yordanova, V. Manolov, Investigation of the possibility of determining the thermal conductivity coefficient of A356 foam by mathematical modeling and identification procedure, J. Chem. Technol. Metall., 57, 4, 2022, 847-856.
16. L.J. Gibson, M.F. Ashby, Cellular Solids: Structure and Properties, Press Synd. of Un. of Cambridge, UK, 1997.
17. B. Parveez, N.A. Jamal, H. Anuar, Y. Ahmad, A. Aabid, M. Baig, Microstructure and Mechanical Properties of Metal Foams Fabricated via Melt Foaming and Powder Metallurgy Technique:A Review, Materials, 15, 15, 2022, 5302. https://doi.org/10.3390/ma15155302
18. Standard ISO 13314, (2011), ISO 13314:2011 - Mechanical testing of metals - Ductility testing - Compression test for porous and cellular metals.
19. Z. Zhang , J. Wang, X. Xia, W. Zhao, B. Liao, B. Hur, The Microstructureand Compressive Properties of Aluminum Alloy (A356) Foams with Different Al-Ti-B Additions, Mat. Sci., 22, 3, 2016, 337-342. https://doi.org/10.5755/j01.ms.22.3.8559